JOURNAL OF MATERIALS SCIENCE 15 (1980) 3122–3128

Analysis of pull-out tests on fibres embedded in brittle matrices

PETER BARTOŠ
Department of Civil Engineering, Paisley College of Technology, Scotland, UK

A graphical interpretation and analysis of pull-out tests is developed to indicate combined effects of factors such as the tensile strength of the fibre and the bond characteristics of the fibre–matrix interfaces on the mode of pull-out failure. In addition to the critical embedment length the significance of two other embedment lengths is shown. One is the minimum length at which a tensile failure of a reinforcing element is not preceded by debonding and the other one is the maximum embedment length at which a complete debonding occurs instantaneously. The graphical analysis is applied to a typical pull-out test result and quantitative values of the ultimate elastic shear bond and the frictional bond are obtained.

1. Introduction

A graphical interpretation of pull-out test results is developed in the present work. The interpretation facilitates an analysis of the pull-out test results and, using an appropriate theoretical model, it enables numerical values of the shear bond and its distribution along the fibres to be determined.

In the first part the graphical interpretation is used to demonstrate the influence of relative magnitudes of ultimate shear flow, Q, frictional flow, q_f, and tensile strength of the fibre T_{fu} on the mechanism and mode of pull-out failure. A shear flow, q, which is the shear force at the interface per unit length of the reinforcing fibre, is used instead of the usual shear bond stress τ_s because it avoids the necessity of determing the surface areas or perimeters of the fibrous reinforcement.

In the second part of this work an example of a practical application of the graphical interpretation is shown. A quantitative analysis is carried out, the mechanism of the pull-out failure is reconstructed and extensions of the fibre during the pull-out tests are determined. The chosen case demonstrates how the values of the critical embedment length L_c and the length L_p at which debonding is no longer instantaneous and complete are obtained from a single test in which a pull-out mode of failure is observed.

2. Graphical interpretation of the pull-out mechanism

Let it be assumed that an elastic shear flow, q, develops along the fibre–matrix interface and increases to $q_{max} = Q$ at which the shear bond fails. Using equations from a theoretical model of the pull-out it is possible to determine a pull-out force, T_q, which generates $q_{max} = Q$ and breaks the shear bond for any given set of test and material parameters and for any embedment length L of the fibre. In this work a model of the pull-out, developed previously by Bartoš [1] and based on a shear-lag analysis similar to that applied by Allen [2], is adopted because it simulates the configuration of a pull-out test as shown in Fig. 1. The force T_q is obtained from the following equation

$$T_q = \frac{Q \sinh \mu L}{\mu \cosh \mu L}, \tag{1}$$

where

$$\mu^2 = \frac{\alpha_c}{\alpha_f \cdot \alpha_m} \tag{2}$$

and

$$\alpha_c = \alpha_f + \alpha_m = A_f E_f + A_m E_m. \tag{3}$$

A_f and A_m are the areas of cross-section and E_f and E_m are the moduli of elasticity of the fibre and matrix respectively and k is shear stiffness of the matrix. The curve OAB in Fig, 2 represents the

0022–2461/80/123122–07$02.70/0

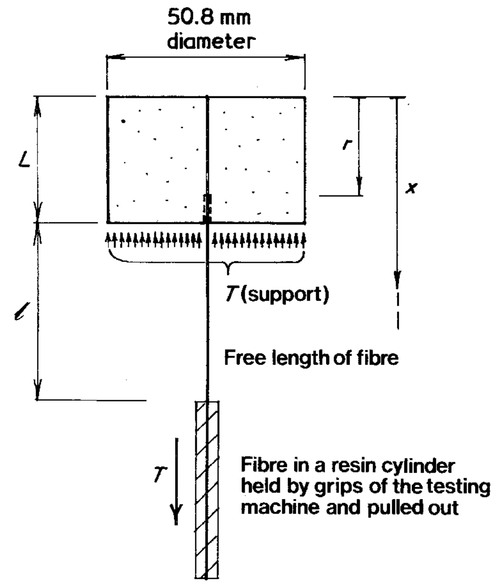

Figure 1 Configuration of a specimen selected for the analysis of pull-out test results. $A_m = 1963\,\text{mm}^2$, $A_f = 2.89 \times 10^{-2}\,\text{mm}^2$.

force T_q plotted as a function of L for constant μ and Q. The behaviour of reinforcement is considered to be elastic an Poisson's effects are neglected.

3. Influence of the strength of fibres and characteristics of the bond on the mode of pull-out failure

3.1. Strong fibres

In this instance, let it be assumed that the tensile strength of the fibre, T_{fu}, which is independent of the embedded length L and of magnitude greater than T_q, is represented by the line EF in Fig. 2. When a pull-out force, T, which is greater than T_q is applied to an embedded fibre the bond fails and debonding can begin. Whether at this instant the fibre also pulls out depends on the frictional bond.

To simplify the analysis, consider that a constant frictional flow, q_f, develops instantly along a debonded interface and it resists a relative displacement between the matrix and reinforcement. When the fibre–matrix interface debonds over a distance, s, the pull-out force available at the point where the debonded interface borders the intact region, r, will be reduced to $T' = T - q_f s$. The frictional flow, q_f, represents the loss of force, T, over a unit length of the debonded interface (Fig. 2). The higher the value of q_f, the higher is the total loss S of the pull-out force occurring along the debonded length s.

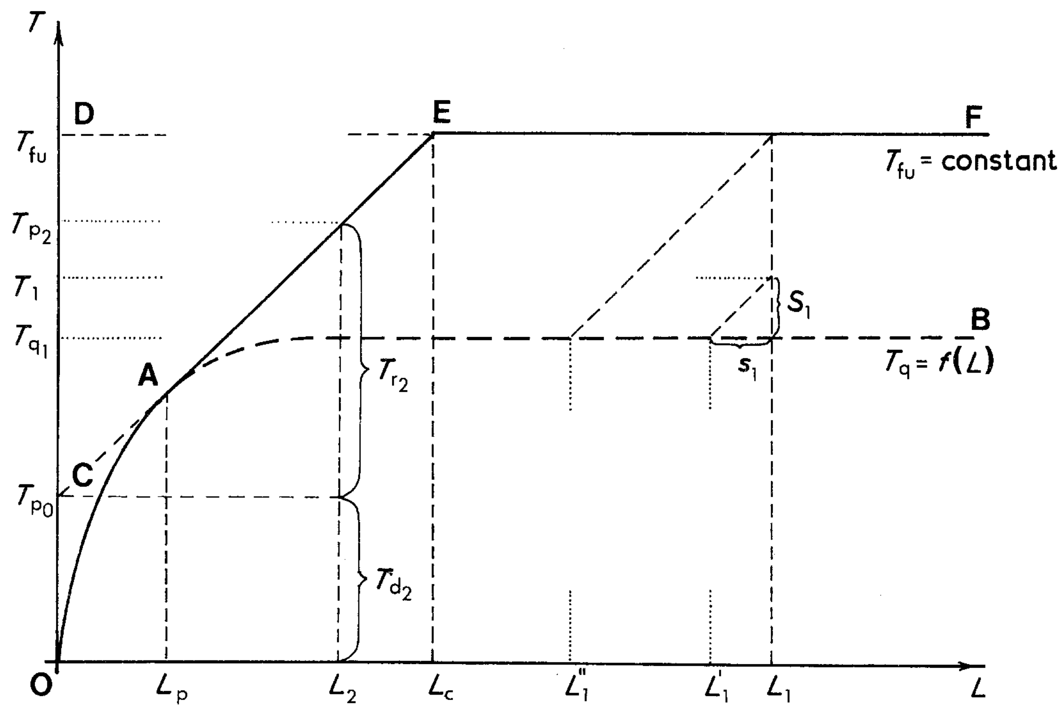

Figure 2 Load–embedment length diagram for a strong fibre with moderate frictional bond and $L > L_p$.

3.1.1. Influence of the embedded length

To illustrate this, consider a fibre of an embedded length, L_1, subjected to a pull-out force T_1 which exceeds the force T_{q1} required for the initial break of the bond (Fig. 2). The excess force $S_1 = T_1 - T_{q1}$ causes the debonding to proceed over a distance of s_1 thus reducing the intact embedded length to $L_1' = L_1 - s_1$. To extend the debonded region s_1 further an increase of the force T_1 is necessary. In this particular case an increase of force, T, extends the region s until $T = T_{fu}$. At this stage the debonded length reaches its maximum and at the same time the fibre fails in tension. The debonded length at the instant of the tensile failure extends from L_1 to L_1''. Fig. 2 shows that the same mode of failure will occur for the pull-out of all embedded lengths longer than the critical embedment length L_c.

For embedment lengths shorter or equal to L_c the pull-out mode changes. When $L_p < L_2 \leqslant L_c$, where L_p is the maximum length at which complete debonding occurs instantaneously, the debonding is faster than in the case of L_1 because with the decrease of the intact bonded length, the force T_q also decreases, but at an increasing rate. For a $T = T_{p2}$ (Fig. 2) the debonded region extends from L_2 to L_p. At this instant the remaining intact embedded length, L_p, debonds without any further increase of the force T and the fibre starts to pull out. The force required to maintain the pull-out immediately reduces to a value of a residual force T_{r2} where

$$T_{r2} = T_{p2} - T_{p0} = q_f L_2. \tag{4}$$

A similar process will take place for all embedded lengths between L_p and L_c. The line AE therefore forms the boundary line for the pull-out failures preceded by gradual debonding. The boundary is a tangent to the curve OAB and its slope is determined by the magnitude of the frictional flow, q_f. The embedded length corresponding to the point E where the line CAE intersects the line DEF is the critical embedment length L_c.

The last possibility to be investigated is the case where $L \leqslant L_p$. Let an embedment length, L_3, be selected and follow the mechanism of the pull-out failure shown in Fig. 3. The rate of decrease of T_q which follows the reduction of the bonded, intact length is now considerably higher than the frictional loss of the pull-out force. This means that when $T = T_{q3}$ the bond is broken and the whole embedded length debonds instantaneously. The magnitude of the force required to maintain the pull-out reduces to $T_{r3} = q_f L_3$. For $L \leqslant L_p$ the ultimate pull-out force T_p does not increase linearly.

It is interesting to note that the instantaneous drop, T_d, in the magnitude of the pull-out force, T_q, which occurs when debonding is complete, remains constant for all embedment lengths in the interval $L_p < L \leqslant L_c$. The force T_{d2} is determined as an intercept, C, of the tangent AE with the vertical axis. It follows that the lower the frictional flow q_f the greater is the instantaneous drop T_d in the magnitude of the pull-out force (Fig. 3).

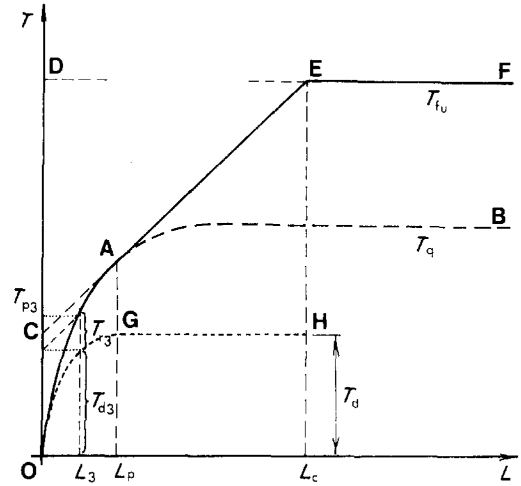

Figure 3 Load–embedment length diagram for a strong fibre with moderate frictional bond and $L \leqslant L_p$.

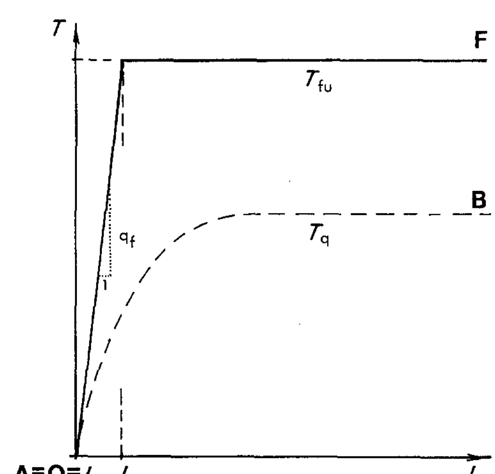

Figure 4 Load–embedment length diagram for a strong fibre with high frictional bond.

3.1.2. Influence of the frictional flow

In this case, the magnitude of the frictional flow is varied whilst the reinforcement remains strong ($T_{fu} > T_q$). A decrease in magnitude of q_f causes an extension of the instantaneous pull-out length, L_p. Note that the point L_p is much less affected than the critical length L_c, which extends rapidly. The ratio of T_r/T_d decreases.

An increase in the magnitude of q_f leads to a reduction of L_p and L_c until L_p merges with the origin (see Fig. 4). In this case the ultimate pull-out force T_p for any embedded length not exceeding L_c depends only on the frictional flow q_f. There will be no instantaneous drop T_d of the pull-out force at the start of the pull-out. Any further increase of, q_f, will cause a further reduction of L_c.

3.2. Weak fibres

Let consideration be given to the case of $T_{fu} < T_q$. Figs. 5a and b show the effects of low or high values of frictional flow q_f. Two modes of failure are identified on the diagram in Fig. 5a. The failure is either a tensile one, without any debonding at all, or it is an instantaneous pull-out failure. The diagram in Fig. 5b illustrates the other extreme case where q_f is very high. Here, for short embedment lengths ($L \leqslant L_c$), the pull-out mode of failure is purely frictional. For $L_c < L \leqslant L_f$ the pull-out changes to a tensile failure. In both cases the failure is preceded by partial debonding. For $L > L_f$ the tensile failure occurs without any debonding at all.

The most complex case occurs for a moderate value of q_f when four modes of failure are identified (see Fig. 5c):

(1) $0 < L \leqslant L_p$ with complete, instantaneous debonding and pull-out;

(2) $L_p < L \leqslant L_c$ with pull-out preceded by debonding;

(3) $L_c < L \leqslant L_f$ with tensile failure preceded by debonding;

(4) $L_f < L$ with tensile failure without debonding.

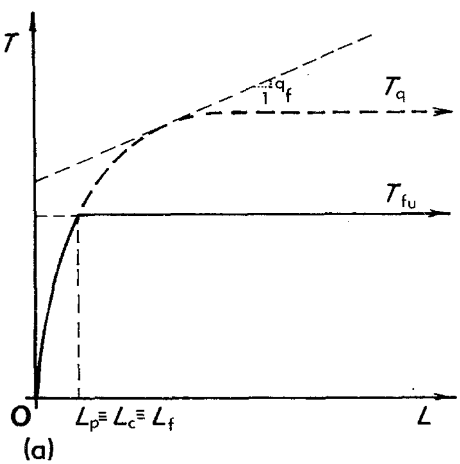

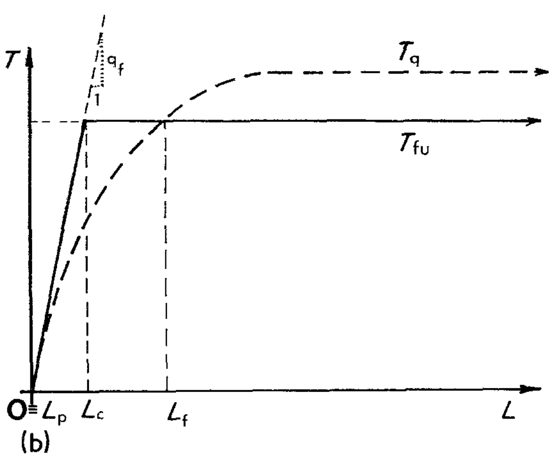

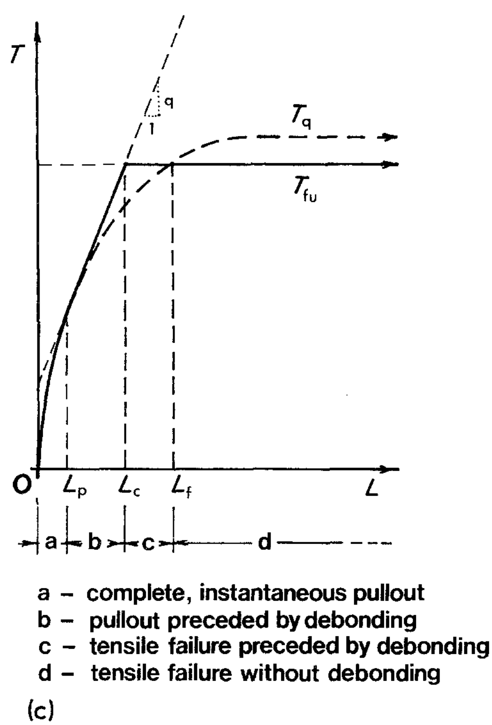

Figure 5 Load–embedment length diagram for a weak fibre with (a) high frictional bond; (b) low frictional bond; (c) moderate frictional bond.

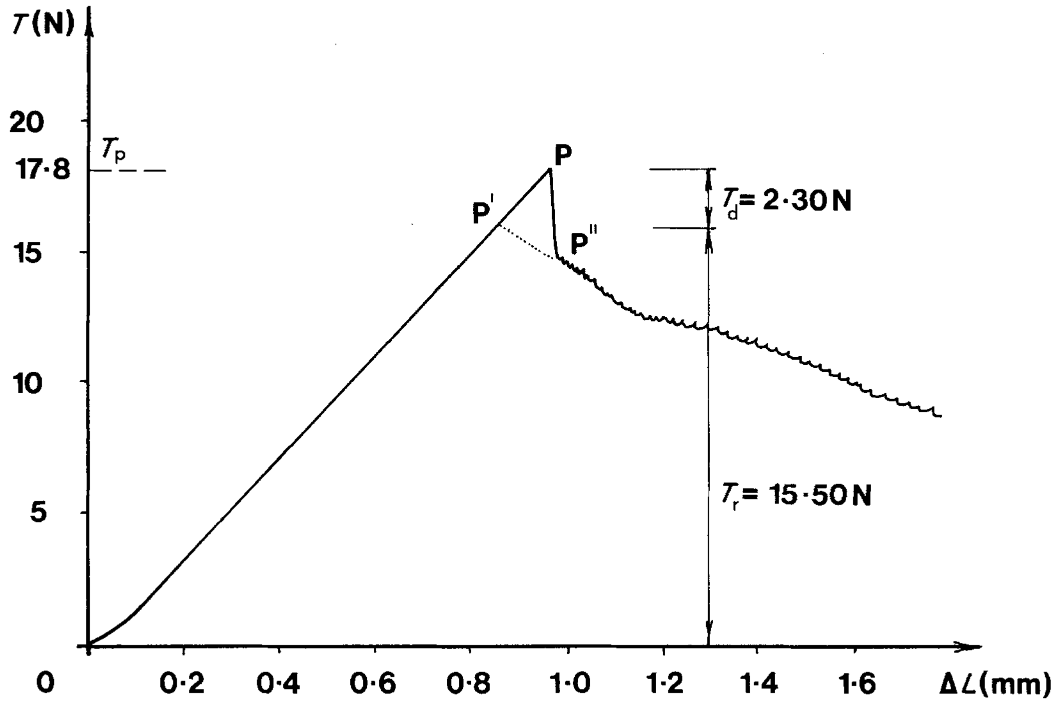

Figure 6 Load–extension diagram. Pull-out test on an E-glass strand in OPC matrix, dry-cured for 7 days (E_m = 7000 N mm^{-2}; E_f = 70000 N mm^{-2}). The configuration of the test is shown in Fig. 1.

4. Application of the analysis to a pull-out test result

In this part, a typical example of a pull-out test result is selected from a series of tests on glass strands embedded in cement-based matrices [3]. Fig. 1 shows the dimensions and general arrangement of the test specimens used. The matrix was a hardened Portland cement paste, the reinforcing element was an E-glass strand. A typical load–extension diagram obtained from a test in which a complete pull-out of the strand was recorded is shown in Fig. 6.

Considering the geometry of the test specimen, the manner in which the load was applied, the existence of frictional flow and using the model of Bartoš [1], the shear flow, q, developed by a pull-out force T at the intact region, r, (Fig. 1) of a partially debonded interface is obtained from the equation

$$q = T - q_f(L-r)\frac{\cosh \mu x}{\sinh \mu r}. \qquad (5)$$

By rearrangement and substituting $T = T_p$, $q = Q$ and $x = r$ gives

$$T_p = \frac{Q}{\mu}\left(\frac{e^{2\mu r}-1}{e^{2\mu r}+1}\right) + q_f(L-r). \qquad (6)$$

When the ultimate shear flow Q is reached but no debonding has occurred yet $r = L$, Equation 1 applies, Equation 2 applies in all cases.

In order to be able to determine the exact mode of failure and to find the ultimate shear flow Q it is necessary to know one of the following factors:

(1) The extent of partial debonding $(L-r)$ which had occurred before the fibre pulled out of matrix or failed in tension;

(2) the shear stiffness, k, of the matrix.

The partial debonding which can occur before a pull-out failure is difficult to measure directly in a composite with an opaque matrix such as cement paste. The debonding also depends on Q and cannot be estimated reliably.

The shear stiffness, k, is likely to remain constant for all tests carried out on one type of specimen with the basic material and physical parameters and properties remaining constant. Once the magnitude of k is known, the whole mechanism of the pull-out failure for a particular case can be established. For our case, using a model of a composite element [2, 3] the shear stiffness $k = 3430$ N and $\mu = 1.3$ mm^{-1}. It is now possible to plot the load–embedment length diagram and to determine the mechanism of the pull-out failure

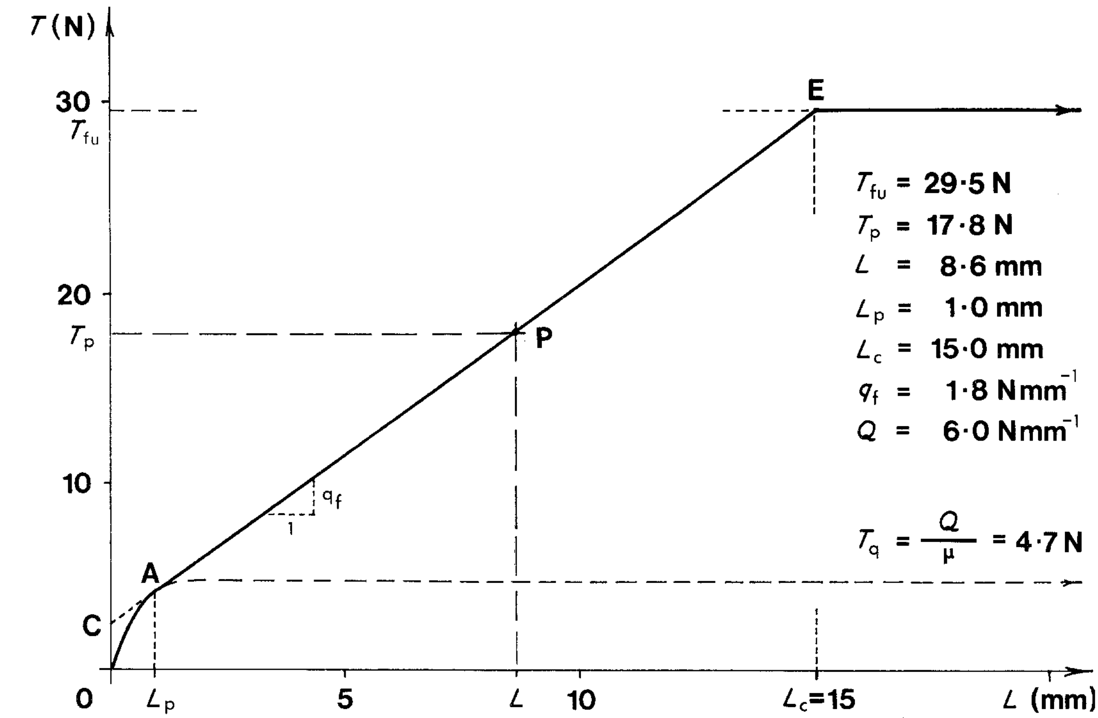

Figure 7 Load–embedment length diagram obtained by analysis of the test result shown in Fig. 6.

(see Fig. 7). Part of the diagram is already known. The average ultimate tensile load of the strand defines the line EF. The frictional flow $q_f = T_r/L = 1.81\,\mathrm{N\,mm^{-1}}$ determines the slope of the line CE passing through the point P which represents the pull-out test result. With the aid of a computer or, less accurately, by a graphical fit the value of Q required for the curve OAB which represents T_q to touch the line CE was determined. For the case discussed $Q = 6.2\,\mathrm{N\,mm^{-1}}$. By plotting the curve $T_q = f(L)$ for $Q = 6.2\,\mathrm{N\,mm^{-1}}$ and $q_f = 1.81\,\mathrm{N\,mm^{-1}}$; the load–embedment diagram shown in Fig. 7 is completed. The mechanism of the pull-out failure is now summarized in Table I.

The corresponding values of critical embedment length and the maximum length at which instantaneous pull-out occurred were $L_c = 15$ mm and $L_p = 1$ mm, respectively.

During the pull-out tests the crosshead of the testing machine moved at a constant rate of displacement. The load–extension diagrams therefore did not record a decrease in the total extension ΔL which occurred immediately after the ultimate pull-out load had been reached. Instead the distance P–P′–P″ as shown in Fig. 6, was traversed instantaneously and the curve showed an almost vertical drop from the peak P to the point P″.

5. Discussion

The interpretation and the analysis of the pull-out mechanism offer an improvement over a traditional method for determination of the critical length L_c. In the current practice a series of pull-out tests in which the embedment length is gradually increased are carried out until tensile failures of the reinforcement are recorded. This method is applicable to matrices and fibres of uniform, homogeneous materials with very small variations in properties

TABLE I Summary of the mechanism of pull-out failure

Pull-out Force, T (N)	Stage of pull-out failure
$0 < T < 4.7$	The entire interface remained intact.
$T = 4.7 = T_q$	The shear flow q reached the value of $Q = 6.2\,\mathrm{N\,mm^{-1}}$ and the bond was broken at the point of entry of the strand into the cement matrix.
$4.7 < T < 17.8$	The debonding gradually extended until only approximately 1 mm of embedded length remained intact.
$T = 17.8 = T_p$	The remaining intact length of interface debonded instantaneously; the strand began to pull out and the pull-out force decreased rapidly.
$T = 15.5 = T_r$	The residual force T_r was initially equal to $q_f L$; it started to decrease as the strand pulled out of the matrix.

of their interfaces. In all other cases the determination of L_c becomes difficult because both pull-outs and tensile fractures are recorded for a considerable interval of embedded lengths. A proper statistical evaluation of the variability of L_c is then impossible [3, 5] and an arbitrary method to determine the critical length L_c has to be adopted. The graphical interpretation shows that a critical length can be established for each individual pull-out test. This is already practicable for results in which the reinforcement pulls out; when a method for a direct measurement of the extent of debonding becomes available it will be possible to determine the L_c from a set of tests irrespective of the mode of failure observed.

In the case of glass fibre reinforced cement the graphical interpretation of the pull-out provides a useful explanation of the causes of a long-term loss of impact resistance and the pseudo-ductility of the composite stored in a moist environment [6]. It shows how the effects of a simultaneous decrease of strength of the fibres and an increase of the shear and frictional bond with time *combine* to cause a dramatic reduction of the L_c value of the fibres. The reduction of L_c and, possibly, even the establishment of a short L_f relative to the length of the fibres, almost eliminates the pull-out mode of failure and, in turn, causes the composite to fail by a single instead of a multiple fracture with a high energy absorption.

In this work the model of Bartoš [1] was used because comparison could then be made with previous pull-out tests [3], however, the graphical interpretation is applicable to models simulating other pull-out test configurations (for example [7, 8]).

6. Conclusions

The graphical interpretation of the pull-out mechanism provides clear definitions of three significant embedment lengths, L_p, L_c, and L_f, at which the modes of failure change. It indicates how these embedded lengths are affected by the strength of reinforcement and by the magnitudes of the shear and frictional bond. Combined with a model simulating the pull-out the interpretation permits the values of the basic bond characteristics to be determined.

References

1. P. BARTOŠ, Ph.D. Thesis, University of Southampton, 1977.
2. H. G. ALLEN, Construction Industry Research and Information Association (CIRIA) Report 55 (1975).
3. P. BARTOŠ, CIRIA Project Record 94/1 (1971).
4. H. L. COX, *J. Appl. Phys.* 3 (1952) 72.
5. J. AVESTON and A. KELLY, *J. Mater. Sci.* 8 (1973) 352.
6. E. COHEN and S. DIAMOND, Proceedings of the International Union of Testing and Research Laboratories for Materials and Structures Symposium on Fibre Reinforced Cement and Concrete, London, September 1975 (Construction Press, Lancaster, UK, 1975), p. 347.
7. A. TAKAKU and R. G. C. ARRIDGE, *J. Phys. D.* 6 (1973) 2038.
8. J. BOWLING and G. W. GROVES, *J. Mater. Sci.* 14 (1979) 431.

Received 21 February and accepted 5 June 1980